UDK 519.61/.64:620.172:677.1/.5
Original scientific article/Izvirni znanstveni članek

ISSN 1580-2949
MTAEC9, 49(4)509(2015)

NON-LINEAR FINITE-ELEMENT SIMULATIONS OF THE TENSILE TESTS OF TEXTILE COMPOSITES

NELINEARNA SIMULACIJA NATEZNIH PREIZKUSOV TEKSTILNIH KOMPOZITOV S KONČNIMI ELEMENTI

Tomáš Kroupa, Kryštof Kunc, Robert Zemčík, Tomáš Mandys

University of West Bohemia in Pilsen, NTIS – New Technologies for the Information Society, Univerzitní 22, 306 14, Plzeň, Czech Republic
kroupa@kme.zcu.cz

Prejem rokopisa – received: 2014-07-25; sprejem za objavo – accepted for publication: 2014-09-15

doi:10.17222/mit.2014.117

The main aim of this paper is to find if it is possible to identify material parameters using only three force-displacement dependencies, each for a different angle between the loading force and the principal material directions. The tested materials are textiles made of epoxy resin and fibers in the form of a glass plain weave, a glass quasi-unidirectional weave, a carbon plain weave, a carbon quasi-unidirectional weave, an aramid plain weave and an aramid quasi-unidirectional weave. The plain weave has theoretically 50 % of the fibers in the first and 50 % in the second principal material direction. The quasi-unidirectional weave has theoretically 90 % of the fibers in the first and 10 % in the second principal material direction. Seven types of specimens for each material were subjected to experimental tests. The first principal material direction of each material forms an angle between 0 ° and 90 ° with a step of 15 ° with the applied loading force. The results show that it is possible to identify the material parameters with sufficient accuracy using only three force-displacement dependencies for five out of six materials.

Keywords: textile composite, cyclic tensile test, material parameters, plasticity, weave locking, identification, optimization

Namen članka je preiskava možnosti ugotavljanja parametrov materiala z uporabo samo treh odvisnosti sila-raztezek pri različnem kotu med silo obremenjevanja in glavno smerjo materiala. Preiskovani materiali so tekstil, izdelan iz epoksi smole in vlaken v obliki platnene vezave, kvazi usmerjene vezave, ogljikove platnene vezave, ogljikove kvazi usmerjene vezave, aramidne platnene vezave in aramidne kvazi usmerjene vezave. Platnena vezava ima teoretično 50 % vlaken v prvi in 50 % v drugi prednostni smeri usmerjenosti materiala. Kvazi usmerjena vezava ima teoretično 90 % v prvi in 10 % v drugi prednostni smeri usmerjenosti materiala. Sedem vrst vzorcev vsakega materiala je bilo preverjeno s preizkusi. Prva glavna usmerjenost pri vseh materialih je bila pod kotom med 0 ° in 90 ° s koraki po 15 ° glede na delovanje sile. Rezultati kažejo, da je bilo mogoče dovolj zanesljivo ugotoviti parametre materiala samo z uporabo treh odvisnosti sila-raztezek pri petih od šestih uporabljenih materialih.

Ključne besede: tekstilni kompozit, ciklični natezni preizkus, parametri materiala, plastičnost, zaklepanje vezave, identifikacija, optimizacija

1 INTRODUCTION

Various kinds of fibrous composite materials are used in modern applications. The main advantages over the classical metallic materials are the beneficial stiffness- and strength-to-mass ratios and the possibility to achieve desired anisotropic mechanical properties wherever necessary. Nevertheless, mathematical models used for designing such structures often require approaches different than those known for classical materials. One of these models is described in this paper. The presented model is kept as simple as possible in the order to keep the number of material parameters as low as possible. It is able to describe the non-linear elastic response, the plastic flow in shear only and the so-called locking of the principal material directions (warp and weft).

The main aim of this paper is to investigate if it is possible to identify material parameters using only three force-displacement dependencies, each for a different angle between the loading force and the principal material directions. The tested materials are the textiles made of epoxy resin and the fibers in the form of a plane weave (GP), a glass quasi-unidirectional weave (GU), a carbon plane weave (CP), a carbon quasi-unidirectional weave (CU), an aramid plane weave (AP) and an aramid quasi-unidirectional weave (AU). The plain weave theoretically consists of 50 % of the fibers in the first and 50 % of the fibers in the second principal material direction; the quasi-unidirectional weave consists of 90 % of the fibers in the first and 10 % in the second principal material direction. Seven types of specimens of each material were subjected to experimental tests. The first principal material direction of each material forms an angle between 0 ° and 90 ° with a step of 15 ° with the applied loading force.

2 SPECIMENS

Figure 1 shows the dimensions of the tested specimens where the investigated area is highlighted. It is the area between the extensometer clips where the elongation Δl of the specimens, the locking angle of the weave and the maximum equivalent plastic strain were measured or calculated.

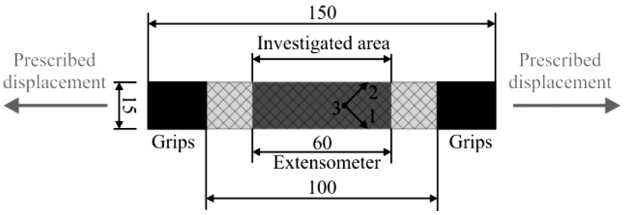

Figure 1: Dimensions of specimens
Slika 1: Dimenzije vzorcev

Table 1 shows the thickness of the specimens of each material.

Table 1: Thickness of specimens
Tabela 1: Debelina vzorcev

Material	Thickness (mm)
GP	1.8
GU	1.8
CP	2.0
CU	1.5
AP	2.2
AU	2.0

2.1 Material model

The model assumes the state of plane stress and the finite-strain theory.

Three coordinate systems are used for the description of the material behavior. General coordinate system $O(x,y,z)$ is used for designating the strains and stresses as $\varepsilon_{xy} = [\varepsilon_x,\varepsilon_y,\varepsilon_{xy}]^T$ and $\sigma_{xy} = [\sigma_x,\sigma_y,\tau_{xy}]^T$. Coordinate system of undeformed configuration $O(1,2,3)$ describes the principal material directions where the strains and stresses are designated as $\varepsilon_{12} = [\varepsilon_1,\varepsilon_2,\varepsilon_{12}]^T$ and $\sigma_{12} = [\sigma_1,\sigma_2,\tau_{12}]^T$. Coordinate system of deformed configuration $O(\xi,\eta,\zeta)$ describes the principal material directions of deformed material configuration and the strains and stresses are designated as $\varepsilon_{\xi\eta} = [\varepsilon_\xi,\varepsilon_\eta,\varepsilon_{\xi\eta}]^T$ and $\sigma_{\xi\eta} = [\sigma_\xi,\sigma_\eta,\tau_{\xi\eta}]^T$ (**Figure 2**). The transformation from system $O(x,y,z)$ to system $O(1,2,3)$ is performed using the rotation about axes $z \equiv e_3$ by angle θ. The strains are transformed using relation $\varepsilon_{12} = T_r\ \varepsilon_{xy}$ [1,2] and the stresses are transformed

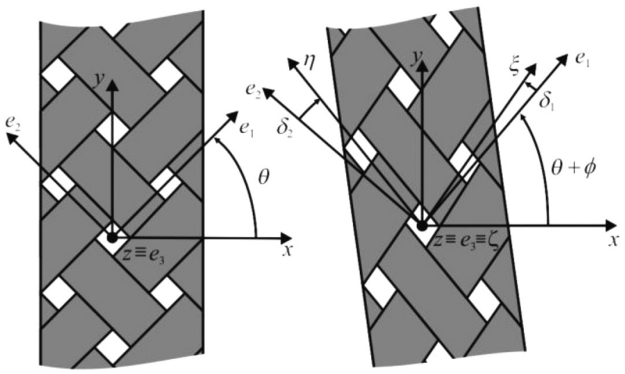

Figure 2: Coordinate systems
Slika 2: Koordinatna sistema

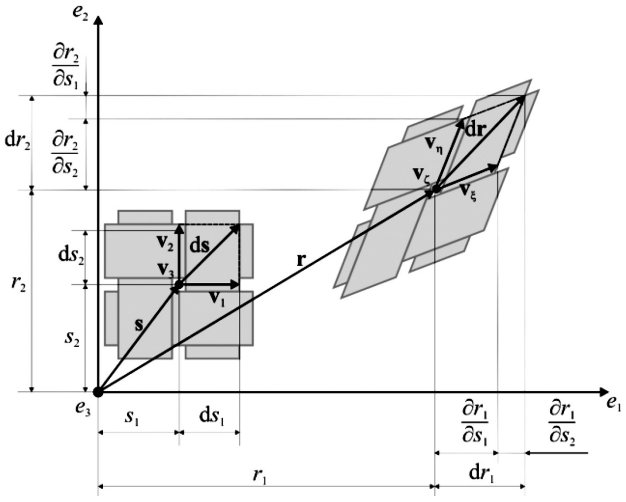

Figure 3: Undeformed and deformed configurations
Slika 3: Nedeformirana in deformirana konfiguracija

using relation $\sigma_{12} = T_r^{-T}\ \sigma_{xy}$ [3] where the transformation matrix has the following form:

$$T_r = \begin{bmatrix} \cos^2\theta & \sin^2\theta & \sin\theta\cos\theta \\ \sin^2\theta & \cos^2\theta & -\sin\theta\cos\theta \\ -2\sin\theta\cos\theta & 2\sin\theta\cos\theta & \cos^2\theta-\sin^2\theta \end{bmatrix} \quad (1)$$

The transformation from system $O(1,2,3)$ to system $O(\xi,\eta,\zeta)$ is performed using deformation gradient:

$$F = \begin{bmatrix} F_{11} & F_{12} & 0 \\ F_{21} & F_{22} & 0 \\ 0 & 0 & F_{33} \end{bmatrix} = \begin{bmatrix} \frac{\partial r_1}{\partial s_1} & \frac{\partial r_1}{\partial s_2} & 0 \\ \frac{\partial r_2}{\partial s_1} & \frac{\partial r_2}{\partial s_2} & 0 \\ 0 & 0 & \frac{\partial r_3}{\partial s_3} \end{bmatrix} \quad (2)$$

which describes the deformation of the representative volume element of the weave (**Figure 3**).

Deformed principal material directions are described using vectors $v_\xi = [F_{12},F_{21},0]^T$ and $v_\eta = [F_{12},F_{22},0]^T$; these are used for defining transformation matrix:[3]

$$T_d = \begin{bmatrix} F_{11}F_{11} & F_{21}F_{21} & F_{11}F_{21} \\ F_{12}F_{12} & F_{22}F_{22} & F_{12}F_{22} \\ 2F_{11}F_{12} & 2F_{21}F_{22} & F_{11}F_{22}+F_{21}F_{12} \end{bmatrix} \quad (3)$$

Subsequently, the transformation of the strains and stresses can be written as $\varepsilon_{\xi\eta} = T_d^{-T}\ \varepsilon_{12}$ and $\sigma_{\xi\eta} = T_d^{-T}\ \sigma_{12}$.

The model is considered in similar way as in[4], with the difference that plasticity is considered in shear only and nonlinearity in material directions ξ and η is modelled as non-linear elasticity. Hence, the stress-strain relation is proposed in the following form:

$$\begin{aligned} \sigma_\xi &= C_{11}\left(1+\frac{k_\xi}{2}\varepsilon_\xi\right)\varepsilon_\xi + C_{12}\varepsilon_\eta \\ \sigma_\eta &= C_{22}\left(1+\frac{k_\eta}{2}\varepsilon_\eta\right)\varepsilon_\eta + C_{12}\varepsilon_\xi \\ \tau_{\xi\eta} &= C_{33}\varepsilon_{\xi\eta}^E \end{aligned} \quad (4)$$

where

$$C_{11}=\frac{E_\xi}{1-\frac{E_\eta}{E_\xi}v_{\xi\eta}^2},\ C_{22}=\frac{E_\eta}{1-\frac{E_\eta}{E_\xi}v_{\xi\eta}^2},\ C_{12}=v_{\xi\eta}\frac{E_\eta}{1-\frac{E_\eta}{E_\xi}v_{\xi\eta}^2}$$

and $C_{33} = 2G_{\xi\eta}$, k_ξ and k_η are non-linear elastic parameters in the ξ and η directions, E_ξ and E_η are the Young's moduli in the ξ and η directions, $G_{\xi\eta}$ is the shear modulus in the composite plane ($\xi\eta$), $v_{\xi\eta}$ is Poisson's ratio in the composite plane ($\xi\eta$), $\varepsilon_{\xi\eta}^{\mathrm{E}}$ is the elastic part of the shear strain. Once the plastic flow is considered in the shear only the remaining strains ε_ξ and ε_η are normal elastic strains (no plastic part exists). The hardening function in the form of the power law is used:

$$\sigma^y=\sigma_0^y+\beta(\bar{\varepsilon}^{\mathrm{P}})^\alpha \tag{5}$$

where σ_0^y is the initial yield stress, α and β are the shape parameters and $\bar{\varepsilon}^{\mathrm{P}}$ is the equivalent plastic strain. As mentioned before, the plastic flow is considered in the shear only, hence, the yield function has the following form:

$$\Phi=\left|\tau_{\xi\eta}\right|-\sigma^y\le 0 \tag{6}$$

And the total shear strain is calculated as

$$\varepsilon_{\xi\eta}=\varepsilon_{\xi\eta}^{\mathrm{E}}+\varepsilon_{\xi\eta}^{\mathrm{P}} \tag{7}$$

Locking angle δ is expressed as the sum of two angles, the first δ_1 is the angle formed by axes e_1 and ξ and the second δ_2 is the angle formed by axes e_2 and η (**Figure 2**).

2.2 FE model

The Abaqus 6.13-4 software is used for finite-element analyses. User subroutine UMAT is used for the implementation of the material model. The size of quadrilateral four-node plane-stress elements is 7.5 mm × 7.5 mm. The Newton-Raphson iteration scheme is used for solving the set of non-linear equations, resulting from the FE discretization.

Subroutines uexternaldb, disp, urdfil are used for controling the cyclic loading process. The process is not trivial due to the high material nonlinearity. The specimens are loaded using the prescribed displacement of the grips and the elongation of a specimen is measured as the elongation of the area between the extensometer grips. **Figure 4** shows the deformed finte-element mesh and the spatial distribution of $\bar{\varepsilon}^{\mathrm{P}}$ for specimen AP 45 °.

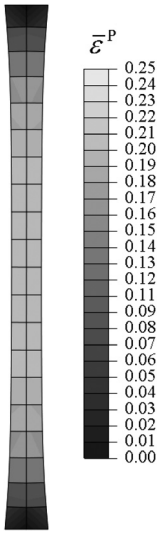

Figure 4: Deformed finite-element mesh with spatial distribution of the equivalent plastic strain for AP 45 °

Slika 4: Deformirana mreža končnih elementov s prostorsko razporeditvijo enakovrednih napetosti za AP 45 °

2.3 Identification

Material parameters are identified using a combination of the finite-element model and experimental data[5]. The differences between the numerically and experimentally obtained force-displacement dependencies are minimized (**Figure 5**). The minimized function is proposed in the following form:

$$r_{\mathrm{L}}=\sum_\theta\sum_{i=1}^{\mathrm{N}}\left(\frac{F^{\mathrm{E}}(\theta,\Delta l_i)-F^{\mathrm{N}}(\theta,\Delta l_i)}{F_{\max}^{\mathrm{E}}(\theta)}\right)^2 \tag{8}$$

where N is the number of the time steps in the finite-element analysis, θ is the angle of the used specimen type in a given identification, Δl_i is the elongation of the specimen in the i-th time step and the denominator is the maximum force in the experiment used as the weight coefficient.

In order to reduce the time consumption, the material parameters are identified in three separate steps.

1. Elastic parameters E_ξ and k_ξ are identified. Only angle θ = 0 ° is taken into account in (8).
2. Elastic parameters E_η and k_η are identified. Only angle θ = 90 ° is taken into account in (8).
3. Elastic parameter $G_{\xi\eta}$ and plastic parameters σ_0^y, β and α are identified. Only angle θ = 45 ° for the materials with the plain weave and θ = 15 ° for the materials with the quasi-unidirectional weave are taken into account in (8).

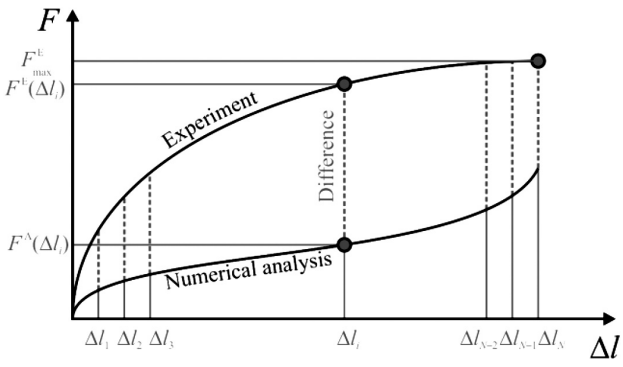

Figure 5: Difference between the finite-element result and the experiment

Slika 5: Razlika med rezultati končnih elementov in preizkusom

Poisson's ratio $v_{\xi\eta}$ cannot be identified using the process mentioned above and must be identified separately. Therefore, the ratio (for each material) was measured using digital image correlation on the 0 ° specimens and was used as a constant in the identification process (**Table 2**).

Table 2: Poisson's ratios
Tabela 2: Poissonovo razmerje

Material	$v_{\xi\eta}$
GP	0.24
GU	0.24
CP	0.19
CU	0.19
AP	0.31
AU	0.31

Table 3: Identified material data
Tabela 3: Ugotovljeni podatki materialov

	GP	GU	CP	CU	AP	AU
E_ξ/GPa	17.7	40.1	51.3	139.4	28.9	48.4
E_η/GPa	17.1	12.6	51.2	8.7	29.9	8.4
k_ξ	–8.8	–11	2.6	–4.2	–13	–0.3
k_η	–25	–88	3.8	–54	–12	–4.8
$G_{\xi\eta}$/GPa	2.2	4.1	3.0	4.1	1.2	1.5
$\sigma_0{}^y$/MPa	15.8	39.8	23.2	13.6	46.1	40.3
β/MPa	74.9	79.6	93.9	102.1	415.8	1585
α	0.23	1.27	0.28	0.26	1.86	2.2

Table 4: Maximum $\bar{\varepsilon}^P$
Tabela 4: Maximum $\bar{\varepsilon}^P$

Material	max($\bar{\varepsilon}^P$)	Specimen angle (°)
GP	0.111	45
GU	0.019	15
CP	0.131	45
CU	0.007	15
AP	0.250	45
AU	0.131	30

Table 5: Locking angle
Tabela 5: Kot zaklepanja

Material	Type of specimen (°)	FEA max (δ) (°)	EXP max (δ) (°)
GP	45	14	15
GU	15	3	4
CP	45	17	26
CU	15	1	10
AP	45	34	35
AU	15	15	20

3 RESULTS

The identified material data (8 parameters) are listed in **Table 3**. **Table 4** shows the maximum values of the equivalent plastic strain calculated in the models and the types of the specimens for which the maximum values were found. A comparison of the locking angles of the weaves calculated in the models and the ones measured in the experiments is in **Table 5**. The results for all analysed materials are shown in **Figures 6** to **13**.

A slight deflection of the tensile dependencies for angles 0 ° and 90 ° is a natural result of the material non-linearity, the hardening and softening, and the fiber-tow entanglement[4].

The resulting force-displacement dependencies for material GP are shown in **Figure 6**. Different shapes of the curves for 0 ° and 90 ° are caused by different numbers of the fibers in the warp (ξ) and weft (η) directions and different levels of the pre-stress of the material are caused by the processes of the entanglement of the weave and the injection of the epoxy matrix. Furthermore, it is not possible to precisely fit the pairs of the curves for 15 °, 75 ° and 30 °, 60 ° due to a large difference in the experimentally obtained results. This can be caused by different levels of damage in the warp and

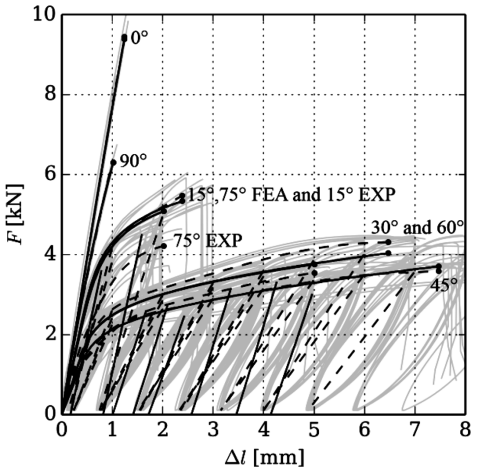

Figure 6: GP (solid line – FEA, dashed line – target/averaged experiments, gray – raw experiments)
Slika 6: GP (polno – FEA, črtkano – ciljna vrednost/povprečje preizkusov, sivo – preizkusi)

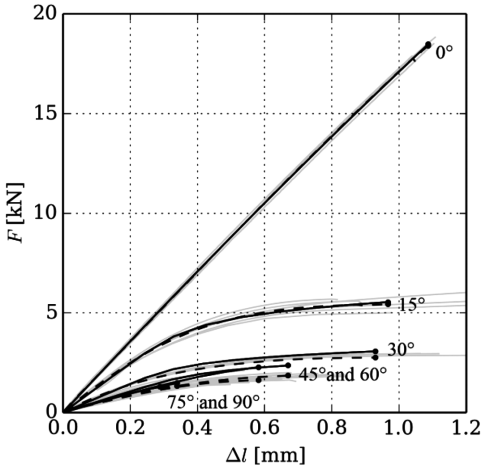

Figure 7: GU (solid line – FEA, dashed line – target/averaged experiments, gray – raw experiments)
Slika 7: GU (polno – FEA, črtkano – ciljna vrednost/povprečje preizkusov, sivo – preizkusi)

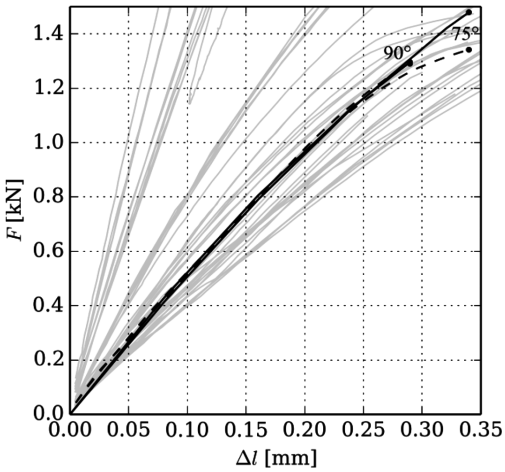

Figure 8: GU zoomed view (solid line – FEA, dashed line – target/averaged experiments, gray – raw experiments)

Slika 8: GU povečan pogled (polno – FEA, črtkano – ciljna vrednost/povprečje preizkusov, sivo – preizkusi)

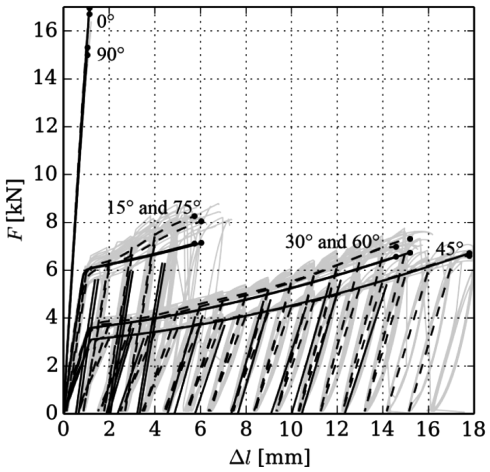

Figure 11: AP (solid line – FEA, dashed line – target/averaged experiments, gray – raw experiments)

Slika 11: AP (polno – FEA, črtkano – ciljna vrednost/povprečje preizkusov, sivo – preizkusi)

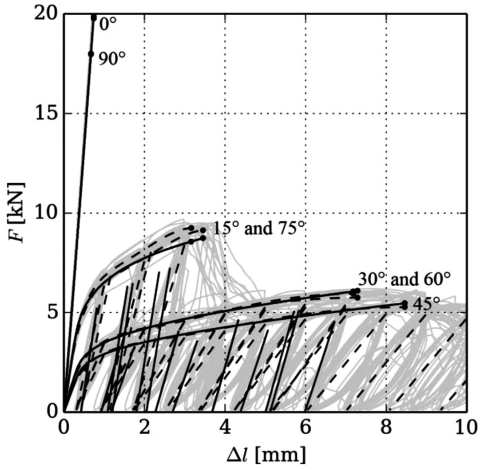

Figure 9: CP (solid line – FEA, dashed line – target/averaged experiments, gray – raw experiments)

Slika 9: CP (polno – FEA, črtkano – ciljna vrednost/povprečje preizkusov, sivo – preizkusi)

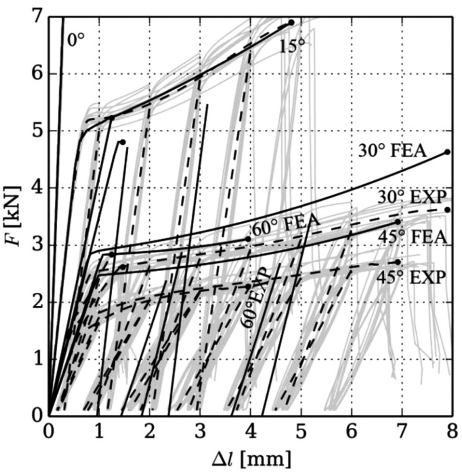

Figure 12: AU zoomed view (solid line – FEA, dashed line – target/averaged experiments, gray – raw experiments)

Slika 12: AU povečan pogled (polno – FEA, črtkano – ciljna vrednost/povprečje preizkusov, sivo – preizkusi)

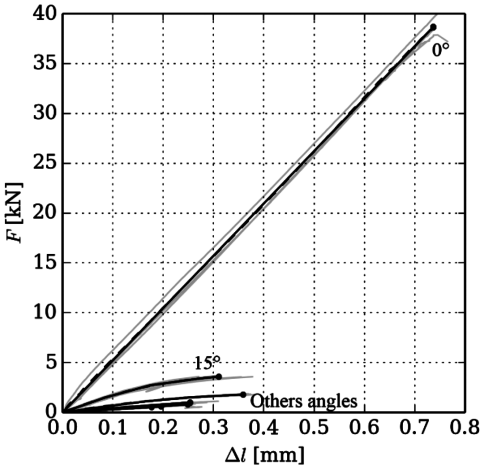

Figure 10: CU (solid line – FEA, dashed line – target/averaged experiments, gray – raw experiments)

Slika 10: CU (polno – FEA, črtkano – ciljna vrednost/povprečje preizkusov, sivo – preizkusi)

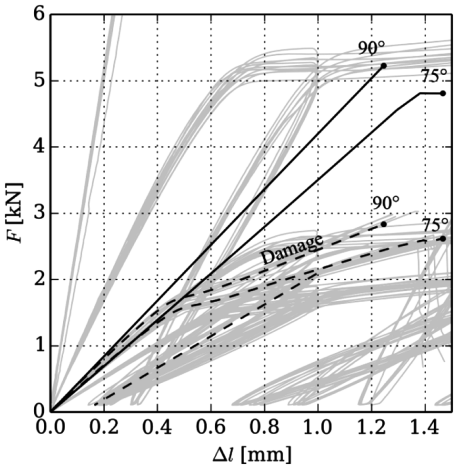

Figure 13: AU zoomed view (solid line – FEA, dashed line – target/averaged experiments, gray – raw experiments)

Slika 13: AU povečan pogled (polno – FEA, črtkano – ciljna vrednost/povprečje preizkusov, sivo – preizkusi)

weft directions that the model is not able to predict in the present state.

The results for GU (**Figure 7**) are fitted on 0 °, 15 ° and 90 °. Nevertheless, even if the curves from the FEA and the experiments for angles 0 ° and 90 ° correspond perfectly, the curves for the other angles do not correspond. The difference between the curves for 75 ° obtained with the FEA and the experiment is shown in **Figure 8**. For comparison, the curve for 90 ° is included in the same graph (**Figure 8**).

We can say that the agreement between the FEA and the experiments for material CP (**Figure 9**) is sufficiently good. Exceptions are the tangents of the unload-load cycles and the impossibility of modeling a tensile test after reaching the maximum force-displacement dependencies (only the black dashed lines in **Figure 9**) that are the consequences of the behavior that is impossible to be captured using the model without damage.

Pure tensile curves without unload-load cycles were measured only for material CU. The results of the FEA show good agreement with the experiments. The results are similar to the ones obtained for the unidirectional carbon-epoxy material made from prepregs.

The best agreement was achieved for material AP (**Figure 11**) where the biggest differences between the FEA and the numerical results were found for 15 ° and 75 °.

The lowest agreement between the FEA and the experimental results was achieved for the AU material. Non-negligible differences are visible for all the unfitted tensile curves, for the unload-load cycles and, unfortunately, even for the 90 ° dependency, where the model is inappropriate for damage modeling.

4 CONCLUSION

A slight deflection of tensile dependencies for angles 0 ° and 90 ° is a natural result of the material nonlinearity, the hardening and softening and the fiber-tow entanglement.

Young's modulus E_1 occasionally differs from E_2. This is caused by an inaccurate ratio of the fibers in the tows in directions ξ and η or by a higher specimen preload in one of the mentioned directions, as a result of the manufacturing technology.

The force-displacement dependencies for the 0 ° and 90 ° specimens are usually non-linear as a result of the fiber-material nonlinearity (stiffening/softening) and the influence of the straightening of the originally wavy fiber tows (stiffening).

It was shown that it is possible to identify the material parameters for five out of six materials using only three force-displacement dependencies with a sufficient accuracy. However, damage modeling or degradation of the elastic material parameters is necessary for more precise simulations of the unload-load cycles.

Future work will be aimed at damage modeling, the compressive behavior of the materials and a precise determination of Poisson's ratios.

Acknowledgement

The work was supported by the European Regional Development Fund (ERDF), through project "NTIS – New Technologies for Information Society", European Centre of Excellence, CZ.1.05/1.1.00/02.0090 and the student research project of Ministry of Education of Czech Republic No. SGS-2013-036.

5 REFERENCES

[1] V. Laš, Mechanics of Composite Materials, University of Bohemia, Plzen 2004 (in Czech)

[2] V. Laš, R. Zemčík, Progressive Damage of Unidirectional Composite Panels, Journal of Composite Materials, 42 (**2008**) 1, 25–44, doi:10.1177/0021998307086187

[3] K. J. Bathe, Finite element procedures, Prentice hall, Upper Saddle River, New Jersey, USA 2007

[4] S. Ogihara, K. L. Reifsnider, Characterization of Nonlinear Behavior in Woven Composite Laminates, Applied Composite Materials, 9 (**2002**), 249–263, doi:10.1023/A:1016069220255

[5] T. Kroupa, V. Laš, R. Zemčík, Improved nonlinear stress–strain relation for carbon–epoxy composites and identification of material parameters, Journal of Composite Materials, 45 (**2011**) 9, 1045–1057, doi:10.1177/0021998310380285